Available online at www.sciencedirect.com

ScienceDirect

Physics Procedia 50 (2013) 177 – 184

Physics Procedia

International Federation for Heat Treatment and Surface Engineering 20th Congress
Beijing, China, 23-25 October 2012

Microstructure and Microhardness of 17-4PH Deposited with Co-based Alloy Hardfacing Coating

D.W.Deng*, C.P.ZHANG, R.Chen, H.F.Xia

School of Materials Science and Engineering, Dalian University of Technology, 116023, Dalian, Liaoning, China

Abstract

Hardfacing is widely used to improve the performance of components exposed to severe service conditions. In this paper, the surface modification was evaluated for precipitation hardening martensitic stainless steel 17-4PH deposited with Co-based alloy stellite12 by the plasma-transferred arc welding (PTAW). The microstructure and microhardness of coating and heat affected zone(HAZ) of base metal were characterized by optical microscope (OM), scanning electron scanning microscope (SEM), X-ray diffractometer and hardness tester. The results show that the interface between weld metal and base metal is favorable without pore and crack, at the same time elements diffusion is observed in the fusion area. However, as the distance from the interface increases, HAZ comprises three different microstructural zones, namely, zones of coarse overheated structures, quenching martensite and martensite, ferrite. The microhardness decreases gradually from the HAZ near interface to the base metal, except the zone of coarse overheated structures. The microhardness of the coating improves a lot and fluctuates in a definitive range, and microstructural gradient is observed including the fusion area (the planar region and the bulky dendrite in a direction perpendicular to the weld interface), the transition zone (the dendrite in a multi-direction way) and the fine grain zone near the surface in the coating (fine equiaxial structure).

Keywords: HAZ, 17-4PH, stellite12, microhardness, microstructure;

1. Introduction

To achieve the purpose of surface strengthening, argon tungsten-arc welding, electrode welding, submerged arc welding and PTAW can be used. The biggest difference among them lies in productivity, dilution and manufacturing cost(Fahimpour, V., S.K. Sadrnezhaad, and F. Karimzadeh;Cordier, A., M. Kleitz, and M.C;Lan, L., et al.;Deng, H.,

* *Emaill*: deng@dlut.edu.cn

doi:10.1016/j.phpro.2013.11.029

H. Shi, and S. Tsuruoka). By using PTAW, the fusion interface is formed between base metal and welding coating with high strength. The microstructure of coating is compact, simultaneously corrosion resistance and wear resistance of coating are excellent. The dilution between base metal and coating reduces, and there is no change in the material properties. Defects, such as porosity, oxide and slag, can hardly be found. At the same time, it not only can reduce the cost, but also can improve the productivity(Jones, M. and U. Waag;Liyanage, T., G. Fisher, and A.P. Gerlich;Liyanage, T., G. Fisher, and A.P. Gerlich;Branagan, D.J., M.C. Marshall, and B.E, 2006).

It is a time of increasing concerns over precipitation hardening stainless steel, because of its excellent corrosion resistance, high strength, high antifatigue and good weldability. 17-4PH, as one of the most well known precipitation hardened stainless steels, with unique properties is widely used in oil, gas and aerospace industries. But workpieces are usually in service in the operation conditions with evolved gases and fast (turbulent) flows, therefore the inner surface of vapor taps made from this steel are always exposed to sequential impacts, high temperature, erosion(Hsiao, C.N., C.S. Chiou, and J.R. Yang, 2002;Das, C.R., et al., 2006;Bhaduri, A.K., et al., 1999;Shoushtari, M.R.T., M.H. Moayed, and A. Davoodi).Obviously, the severe service conditions ask for more excellent surface properties, and hardfacing is widely used to improve the performance of components. Co-base alloys with wear and corrosion resistant is regarded as candidate materials for surface hardening of 17-4 PH stainless steel(Hongxia, D., S. Huiji, and S. Tsuruoka;Jeshvaghani, R.A., M. Shamanian, and M. Jaberzadeh;Gholipour, A., M. Shamanian, and F. Ashrafizadeh).Although precipitation hardened stainless steel is widely used in industry, but the research report on 17-4PH deposited with Co-based alloy by the plasma-transferred arc welding (PTAW) could be rarely found. In this paper, the microstructure and microhardness of 17-4PH deposited with stellite12 was studied.

2. Experimental procedure

The shaft sleeve of precipitation hardening martensitic stainless steel 17-4PH was deposited with Co-based alloy stellite12 by PTAW. The chemical composition of stellite12 alloy and 17-4PH was shown in Table1 and Table2, the PTAW process parameters were provided in Table3. The shaft sleeve, which was deposited with Co-based alloy, was cut into 15×15×15mm samples.

Table 1 The chemical composition of base metal

element	C	Si	Mn	P	S	Ni
Content (%)	<=0.07	<=1.00	<=1.00	<=0.04	<=0.03	3-5
element	Cr	Mo	Cu	N	else	
Content(%)	15-17.5	-	3-5	-	Nb0.15-0.45	

Table 2 The chemical composition of coating

element	C	Si	Mn	Cr	W	Fe
Content (%)	1.4	1.45	1.00	29.5	8.25	3
element	Mo	Ni	Co			
Content(%)	1	3	bal			

Table 3 Welding parameters used in PTAW process

Welding current	Powder feeding rate	Arc oscillation width	Operating voltage	Plasma gas flux, rate	protective gas flux, rate
160A	25g/min	25mm	24-25V	2.5 1/min	12 1/min

The microstructure of base metal, HAZ and coating was described by optical microscopy (OM) and scanning electron microscope (SEM); chemical phases were detected by X-ray diffraction (XRD); the distribution trend of main elements was analyzed by SEM equipped with energy dispersive spectroscopy (EDS); the hardness value was measured by Vickers hardness tester (500g,15s).

3. Experimental procedure

1.1. Microstructures of the coating and HAZ

Fig.1 shows microstructures of the coating and HAZ observered by SEM. Precipitation hardening martensitic stainless steel 17-4PH is sensitive to heat treatment, therefore Fig.1.(a-c) shows obvious microstructural gradient at HAZ due to welding heat input and welding cold cycle after PTAW. HAZ comprises three different microstructural zones, namely, zones of coarse overheated structures, quenching martensite and martensite and ferrite. The grains near the interface grew badly for the high temperature, so the coarse martensites formed at the zone of coarse overheated structures (Fig1.a). With the increased distance from the interface, the temperature decreased but still above austenitizing temperature, so quenching martensite with the prior austenite crystal boundary formed (Fig1.b). As the distance increased further, the temperature declined sharply, therefore there were few ferrites dissolving in austenites due to rapid heating. Because it was at high temperature tempering, austenites were transformed into tempered martensites with rapidly quenching. And there were still existing residual ferrites (Fig1.c).

As the distance from the interface changed, microstructural gradient of the coating was observed including the fusion area (the planar region and the bulky dendrite in a direction perpendicular to the weld interface), the transition zone (the dendrite in a multi-direction way) and the fine grain zone near the surface in the coating (fine equiaxial structure). In the fusion area, a planar growth pattern can be observed near the interface, because of the high gradient of temperature and small constitutional supercooling along the solid–solution interface. As the distance to the interface increased, bulky dendrite appeared with the direction perpendicular to the interface and parallel to the heat flow direction (Fig1.d). In the transition zone, the dendritic structure was still observed. As the result of the decreased temperature gradient and increased constitutional supercooling, the size of dendrites became smaller and smaller with increased distance from the interface. However, because of the multi-directional heat loss, the direction of the dendritic in this area was in a multi-direction way (Fig1.e). With the increased distance, the temperature gradient in the solution became smaller and the constitutional supercooling became higher gradually, so after the transition area the formation of the fine grain zone with a multi-directional growth occurred (Fig1.f).

Though microstructural gradient of the coating was obviously observed, all of the three areas were composed of the dendritic and the interdendritic eutectic structure (Fig.2). And the interdendritic eutectic structure existed in three different forms, they are, respectively, rodlike structure, rosette structure and punctuate structure (Fig.3).

Fig.4 presents the result of XRD analysis of the coating. Co-rich γ phase solid solution, carbides Cr7C3 and Cr23C6 were observed. In addition, the percentage composition of the main elements Co, Fe, Cr, C, Ni and W of the coating was also analyzed (Table4). The amounts of Co and Fe were higher in the dendrite than that in the interdendritic structure, while the interdendritic structure contained larger amounts of Cr and C. Moreover, the percentage composition of the main elements in the three different interdendritic structure was discriminative. Therefore, according to the analysis of chemical phases and element percentage composition, the microstructure was primarily described as Co-rich γ phase dendritic structure with a network of chromium carbides Cr7C3 and Cr23C6 in the interdendritic areas.

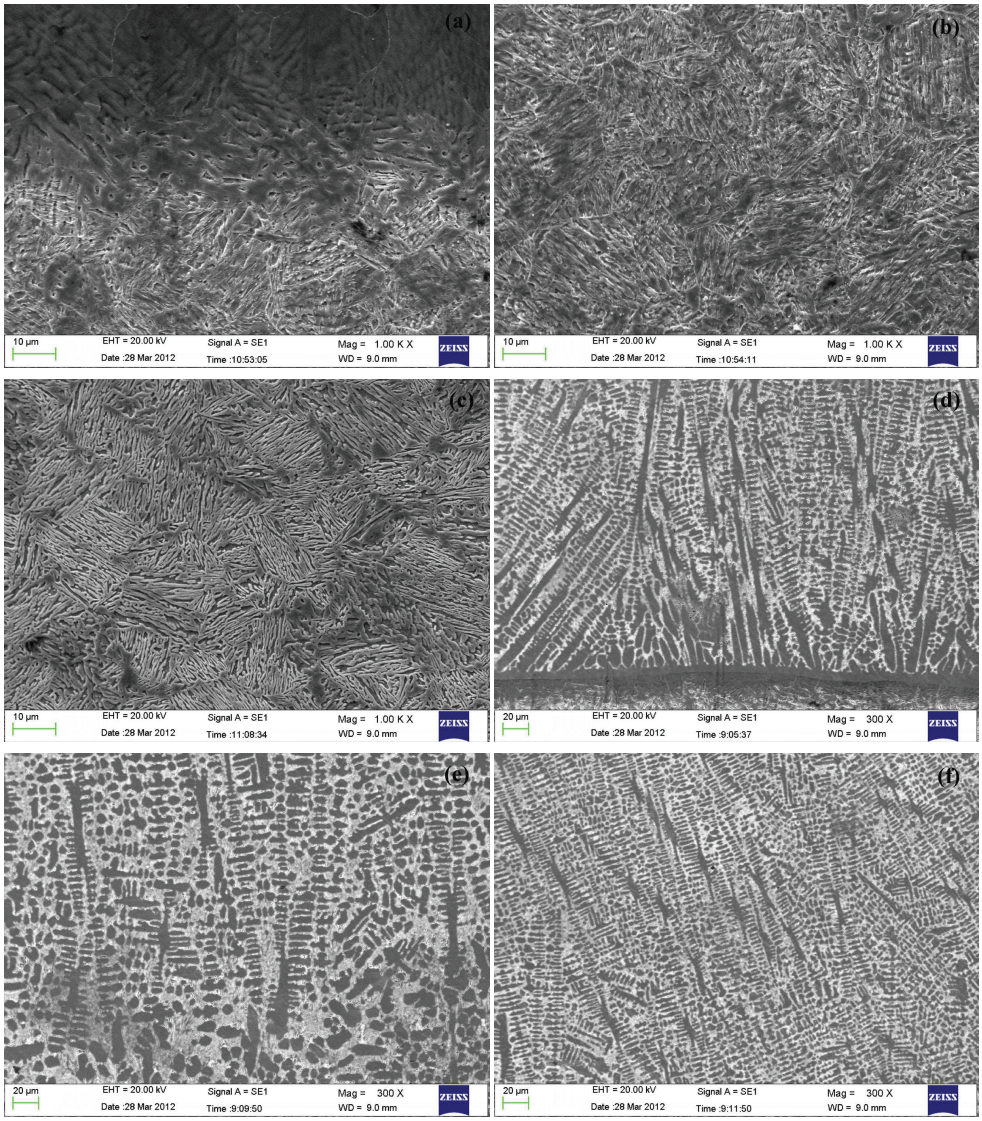

Fig.1.SEM image of HAZ and coating: (a) coarse overheated structures area; (b) quenching martensite area; (c) martensite and ferrite area; (d) the planar and directive dendrite area; (e) the transition zone; (f) the fine grain zone

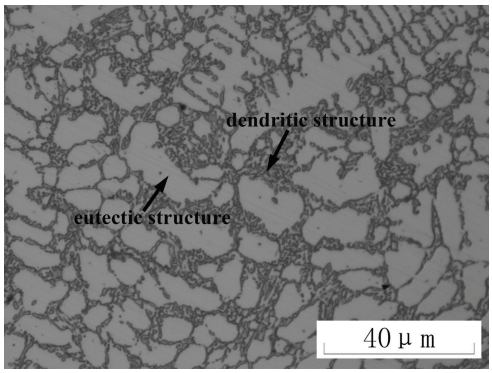

Fig.2.Microstructure of the coating

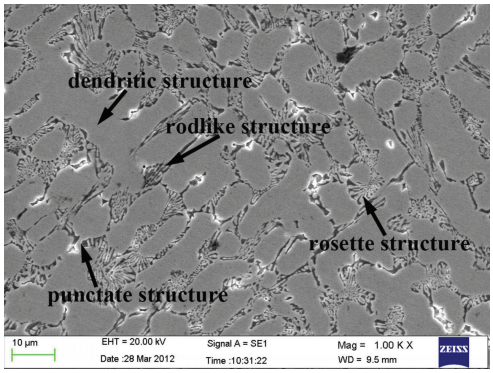

Fig.3.SEM image of the coating

Table 4 Chemical composition of Co-rich dendrite structure and three types of eutectic structure, measured EDS

mass percent(%)	Co	Cr	Fe	W	Si	C
dendritic structure	62.69	24.70	3.66	7.05	1.20	1.22
Rodlike structure	46.52	31.99	2.54	10.63	1.09	7.23
Punctate structure	42.37	35.37	2.27	10.37	0.97	8.64
Rosette structure	45.36	30.35	2.58	8.87	1.17	8.22

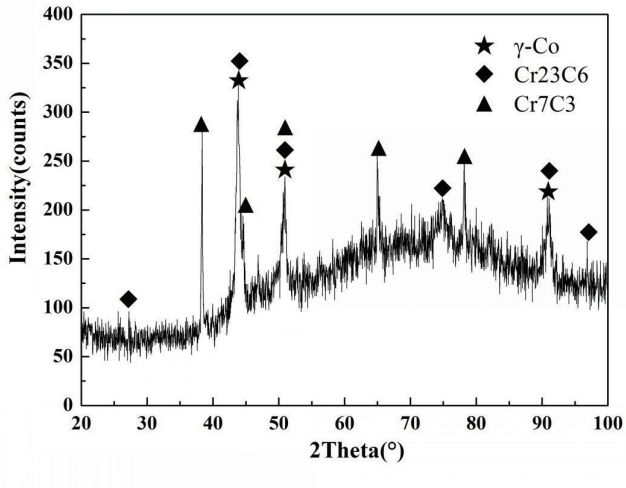

Fig.4.The XRD pattern of the coating

1.2. Microstructure and element distribution of the interface

Fig. 5 shows the interface between stellite12 cladding and 17-4PH. A good interface appearance and a relatively homogeneous structure were obtained by the PTAW without porosities or cracks. The reason was that the high concentration gradient of the interface led to a strong elemental diffusion which resulted in the strong adherence between the base metal and the coating. In addition, this type of boundary was formed, in which grain boundaries from the boundaries within the base metal and then grew in a direction perpendicular to the weld interface into the weld pool. This kind of growth was called epitaxial growth. The evolution of such growth was as a result of

similarities in crystal structure and chemical composition. Line scanning was carried out to investigate dilution of the coating by substrate (Fig.5). As can be seen, the content of Fe, Co and Cr changed a lot in the interface.

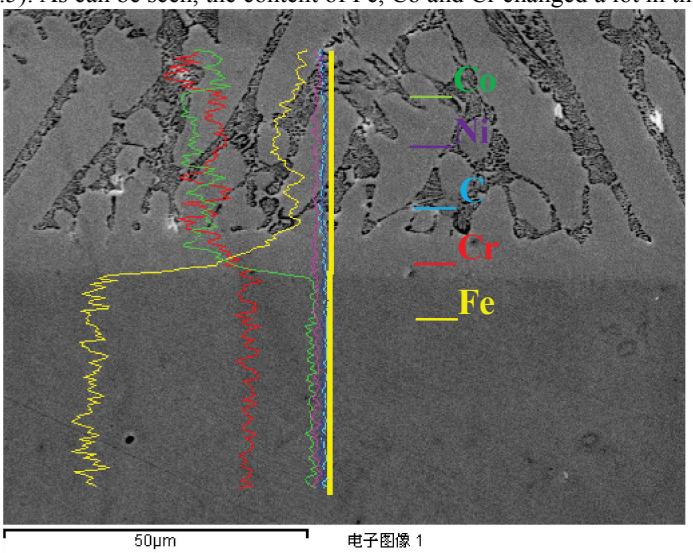

Fig.5. SEM image of the fusion area

1.3. Microhardness of HAZ and coating

Fig.6 presents the Vickers hardness profile of the cross section from the base metal to the coating. As can be seen, the hardness of the base metal, which was not affected by the welding heating cycle, was almost constant and the average value was 296.7HV. There was an obvious gradient of microhardness in the HAZ. The hardness of HAZ near the interface was lowest due to the coarse overheated structures. However, as the distance increased from the interface, solution strengthening turned up with the formation of the quenching martensite. Therefore, the hardness increased. But as the distance increased farther, the hardness decreased because of lower effect of the solution strengthening.

The hardness of the coating near the interface was extremely low as a result of dilution effect by Fe from the base metal. There was a relatively large increase in hardness from the fusion area to the transition area as a result of that the dilution effect weakened and finally vanished. However, since it was commonly accepted that there was a great connection between the microstructure and Vickers hardness, the inhomogeneity of microstructure resulted in fluctuation of hardness in the transition area. And there was an increase in hardness from the transition area to the fine grain area, which can be explained by the evolution of microstructure (If the phase composition was the same, a finer microstructure generally brought about a higher hardness) (Fig.1.e and f). The hardness of the fine grain area was almost constant and about 500HV on average, which was much bigger than that of base metal.

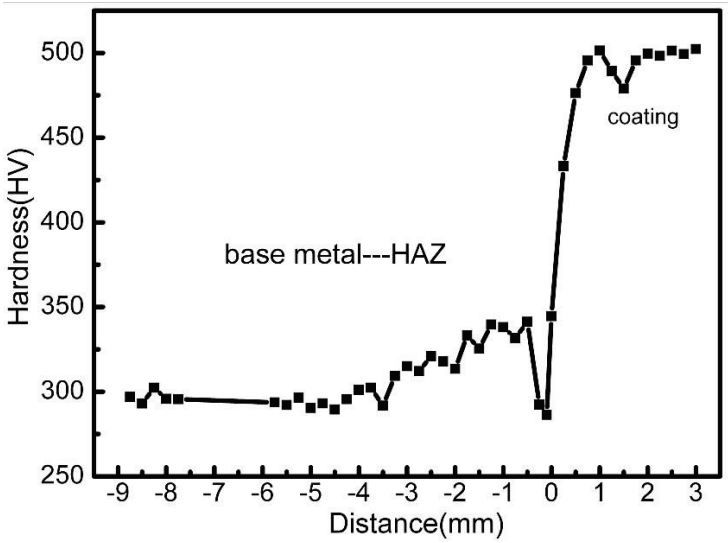

Fig.6. Variations of microhardness from base metal to coating

4. Conclusions

In this paper, the microstructure characteristics of HAZ and coating was first described and analyzed. The as-welded mechanical property was then clarified in terms of the Vickers hardness. The results and conclusions were summarized as follows:

(1) The interface between weld metal and base metal was favorable without pore and crack, and elements diffusion was observed in the fusion area.

(2) HAZ comprised three different microstructural zones, namely, zones of coarse overheated structures, quenching martensite and martensite and ferrite.

(3) Microstructural gradient of coating was observed including the fusion area (the planar region and the bulky dendrite in a direction perpendicular to the weld interface), the transition zone (the dendrite in a multi-direction way) and the fine grain zone near the surface in the coating (fine equiaxial structure).

(4) Microhardness reduced gradually from the HAZ near interface to the base metal except the zone of coarse overheated structures. And the microhardness of the coating improves a lot relative to the base metal. The microhardness of the fusion area is lowest among the three areas. The microhardness of the transition zone fluctuates in a definitive range. The microhardness of the fine grain zone is stable.

Acknowledgements

This work was carried out with the financial support from the National Key Basic Research and Development Program（No.2011CB013402). The author would like to thank Ge Yanliu for his invaluable discussions during the course of the research.

References

Fahimpour, V., S.K. Sadrnezhaad, and F. Karimzadeh, Corrosion behavior of aluminum 6061 alloy joined by friction stir welding and gas tungsten arc welding methods. Materials & Design. 39: p. 329-333.

Cordier, A., M. Kleitz, and M.C. Steil, Welding of yttrium-doped zirconia granules by electric current activated sintering (ECAS): Protrusion formation as a possible intermediate step in the consolidation mechanism. Journal of the European Ceramic Society. 32(8): p. 1473-1479.

Lan, L., et al., Analysis of martensite-austenite constituent and its effect on toughness in submerged arc welded joint of low carbon bainitic steel. Journal of Materials Science. 47(11): p. 4732-4742.

Deng, H., H. Shi, and S. Tsuruoka, Influence of coating thickness and temperature on mechanical properties of steel deposited with Co-based alloy hardfacing coating. Surface and Coatings Technology. 204(23): p. 3927-3934.

Jones, M. and U. Waag, The influence of carbide dissolution on the erosion-corrosion properties of cast tungsten carbide/Ni-based PTAW overlays. Wear. 271(9-10): p. 1314-1324.

Liyanage, T., G. Fisher, and A.P. Gerlich, Microstructures and abrasive wear performance of PTAW deposited Ni-WC overlays using different Ni-alloy chemistries. Wear. 274: p. 345-354.

Liyanage, T., G. Fisher, and A.P. Gerlich, Influence of alloy chemistry on microstructure and properties in NiCrBSi overlay coatings deposited by plasma transferred arc welding (PTAW). Surface & Coatings Technology. 205(3): p. 759-765.

Branagan, D.J., M.C. Marshall, and B.E, 2006. Meacham, High toughness high hardness iron based PTAW weld materials. Materials Science and Engineering a-Structural Materials Properties Microstructure and Processing. 428(1-2): p. 116-123.

Hsiao, C.N., C.S. Chiou, and J.R. Yang, 2002. Aging reactions in a 17-4 PH stainless steel. Materials Chemistry and Physics. 74(2): p. 134-142.

Das, C.R., et al., 2006. Weldability of 17-4PH stainless steel in overaged heat treated condition. Science and Technology of Welding and Joining. 11(5): p. 502-508.

Bhaduri, A.K., et al., 1999. Optimised post-weld heat treatment procedures and heat input for welding 17-4PH stainless steel. Science and Technology of Welding and Joining. 4(5): p. 295-301.

Shoushtari, M.R.T., M.H. Moayed, and A. Davoodi, Post-weld heat treatment influence on galvanic corrosion of GTAW of 17-4PH stainless steel in 3.5%NaCl. Corrosion Engineering Science and Technology. 46(4): p. 415-424.

Hongxia, D., S. Huiji, and S. Tsuruoka, Influence of coating thickness and temperature on mechanical properties of steel deposited with Co-based alloy hardfacing coating. Surface & Coatings Technology. 204(23).

Jeshvaghani, R.A., M. Shamanian, and M. Jaberzadeh, Enhancement of wear resistance of ductile iron surface alloyed by stellite 6. Materials & Design. 32(4): p. 2028-2033.

Gholipour, A., M. Shamanian, and F. Ashrafizadeh, Microstructure and wear behavior of stellite 6 cladding on 17-4 PH stainless steel. Journal of Alloys and Compounds. 509(14): p. 4905-4909.